SF2A 2018
P. Di Matteo, F. Billebaud, F. Herpin, N. Lagarde, J.-B. Marquette, A. Robin, O. Venot (eds)

THE VIMOS PUBLIC EXTRAGALACTIC REDSHIFT SURVEY (VIPERS): THE SUPER-SOLAR METALLICITY MEASURED FOR MASSIVE PASSIVE GALAXIES

M. Siudek[1,2,3], K. Malek[3] and A. Pollo[3,*4]

Abstract. We study the influence of difference in stellar metallicity on the estimated value of redshift of formation of red passive galaxies in VIPERS survey. We derived the stellar mass-metallicity relation for SDSS red passive galaxy sample and found a slightly super-solar metallicity ($log(Z/Z_{\odot}) \sim 0.1$) for massive passive galaxies ($> 10^{11}$ M$_{\odot}$). While the effect of metallicity variations on the estimation of the epoch of the last starburst for low-mass galaxies is negligible, it result in an overestimation of redshift of formation (on average of the order of $10 - 15\%$ but it can be even doubled for low-redshift galaxies) of massive red passive galaxies.

Keywords: galaxies: formation galaxies: evolution galaxies: stellar content

1 Introduction

The estimation of stellar ages in passive galaxies is commonly based on the assumption of their solar metallicity (e.g. Kauffmann et al. 2003; Moresco et al. 2010), although the stellar mass-metallicity relation indicates that metallicities of galaxies increase with their increasing stellar masses (e.g. Gallazzi et al. 2005, 2014). This is a consequence of the inability to unambiguously distinguish the age and metallicities effects, which is known as the age-metallicity degeneracy (Worthey 1994). However, there are some relatively metal-insensitive spectral features (like Balmer lines, Worthey 1994; Jones & Worthey 1995), which allow to mitigate the problem of the age-metallicity degeneracy. Unfortunately, some Balmer lines, like $H\beta$ are difficult to measure accurately in most massive passive galaxies (e.g. Gonzalez-Gonzalez 1993). The reason is that the $H\beta$ feature is often filled by emission from ionized hydrogen, and the systematics of this effect as a function of metallicity are unknown, what increases the uncertainty of the age determined making use of this line. Hence, higher order Balmer lines, like $H\delta$, are more useful as age indicators, as they are less affected by emission than the $H\beta$ line (e.g. Osterbrock 1989) and less diluted by light from red giants (Worthey & Ottaviani 1997). Thus, a realistic spread of metallicities or at least high order Balmer lines should be included in the models for better age and metal discrimination. Gallazzi et al. (2005) derived stellar masses, ages, and metallicities for SDSS galaxies based on the Monte Carlo libraries of star formation histories applied to (Bruzual & Charlot 2003, later BC03) simple stellar population models and analyzed an optimally-selected set of stellar absorption features with distinct sensitivity to age and metallicity. These features include, among others, high-order Balmer lines and the metal-sensitive indices: $[Mg_2Fe]$ (Bruzual & Charlot 2003) and $[MgFe]'$ (Thomas et al. 2003), which allow to remove the dependence on the abundance ratio (Gallazzi et al. 2005).

Building on the stellar properties derived by Gallazzi et al. (2005, 2014) we estimated the stellar mass-metallicity relation for a sample of local SDSS red passive galaxies. Assuming that the stellar mass-metallicity relation does not evolve with cosmic time (Carson & Nichol 2010; Toft et al. 2012; Gallazzi et al. 2014) and

*on behalf of the VIPERS Team, whose members are presented at the end of this proceedings

[1] Institut de F'isica d'Altes Energies (IFAE), The Barcelona Institute of Science and Technology, 08193 Bellaterra (Barcelona), Spain

[2] Center for Theoretical Physics, Al. Lotnikow 32/46, 02-668 Warsaw, Poland

[3] National Centre for Nuclear Research, ul. Hoza 69, 00-681 Warszawa, Poland

[4] Astronomical Observatory of the Jagiellonian University, Orla 171, 30-001 Cracow, Poland

it can be applied to galaxies at $z > 0.5$, we show how neglecting even a small difference in stellar metallicity may change the estimation of stellar ages of VIPERS red passive galaxies. In Sect. 2 we describe SDSS and VIPERS samples of red passive galaxies used for the presented analysis. The description of spectral features and models is given in Sect. 3. The influence of stellar metallicity on redshift of formation is derived in Sect. 4 and summarized in Sect. 5.

2 Data

2.1 VIPERS red passive galaxies

Our work is based on the galaxy sample from the VIMOS Public Extragalactic Redshift Survey (VIPERS, Guzzo et al. 2014). In total almost 100,000 galaxies brighter than $i'_{AB} = 22.5$ were observed in the redshift range $0.4 < z < 1.1$ over an area of ~ 23.5 deg^2 Spectroscopic observations were carried out with the VIsible Multi-Object Spectrograph (VIMOS; Le Fèvre et al. 2003) mounted on the ESO Very Large Telescope, using the multi-object spectroscopy (MOS) mode with the low-resolution red grism ($\lambda_{\rm blaze} = 5810$Å, R = 230, 1$''$ slit) yielding a spectral coverage between 5500 and 9500Å with an internal dispersion of 7.14Å pixel^{-1} (Scodeggio et al. 2005, 2018). The analysis presented in this paper is based on the VIPERS internal data release version 5, which contains 88% spectroscopic measurements of the final sample, presented in details in Siudek et al. (2017).

The sample of 8,174 red passive galaxies was selected based on the variable cut in $U - V$ color evolving with redshift (Fritz et al. 2014). The sample was further pruned to high-quality spectra without sky residuals and with high confidence in redshift measurements over redshift range $0.4 < z < 1$. This led us to a sample of 3,991 red passive galaxies. For details of our sample selection see Siudek et al. (2017).

2.2 SDSS red passive galaxy sample

The analysis presented in this work is based on the publicly available MPHA-JHU DR4 release of spectral measurements of SDSS galaxies (Gallazzi et al. 2005)[1]. The selection of red passive galaxies is based on the lack of star formation activity signatures in the spectrum, i.e., on the absence of an emission $H\alpha$ line in the spectrum. We selected 11,968 high-quality spectra of old, passive galaxies similar to the VIPERS ones. The vast majority (99%) of these SDSS passive galaxies have $D4000_n$ greater than 1.5, which is an independent confirmation that the $H\alpha$ criterion is sufficient to select passive, red galaxies excluding galaxies with recent episodes of star formation.

3 Methodology

In this paper, we adopted a narrow definition of $D4000$ (Balogh et al. 1999, hereafter $D4000_n$) defined as the ratio between the continuum flux densities in the red band (4000-4100Å) and blue band (3850-3950Å). For the $H\delta$ line we used the wider A-$H\delta$ Lick index ($H\delta_A$) definition given by Worthey & Ottaviani (1997). The absorption line strength is obtained by comparing measurements of the spectral flux in the central feature bandpass and two flanking pseudo-continuum regions. For the $H\delta_A$ index the feature range is 4083.50 - 4122.25Å, the blue continuum range is 4041.60 - 4079.75Å, and the red continuum range is 4128.50 - 4161.00Å.

We measured spectral features on 32 stacked spectra of VIPERS red passive galaxies in narrow redshift and stellar mass ($M_{\rm star}$) bins. Spectra were co-added within six $M_{\rm star}$ bins over the range of 10< log($M_{\rm star}$) <12 and six redshift bins over the range of $0.4 < z < 1.0$, to make possible the measurement of $H\delta$ line possible (details see in Siudek et al. 2017).

For the grid of the BC03 model spectra, we derived the nominal $D4000_n$ and $H\delta_A$-stellar age relations with metallicities, $log(Z/Z_\odot) = 0.4$, $log(Z/Z_\odot) = 0.0$, $log(Z/Z_\odot) = -0.4$, and $log(Z/Z_\odot) = -0.7$ (see Fig. 1). The synthetic spectra were generated using the Chabrier initial mass function, Padova 1994 stellar evolutionary tracks and the high-resolution STELIB spectral library downgraded to the typical VIPERS spectral resolution (14$\mathring{A}$) with a star formation history assumed to be a single burst with a timescale $\tau = 0.1, 0.2, 0.3$ Gyr. For each value of τ, a set of synthetic spectra was obtained for stellar ages in the range from 1 to 10 Gyr, with steps of 0.25 Gyr.

[1] `http://wwwmpa.mpa-garching.mpg.de/SDSS/DR4/index.html`

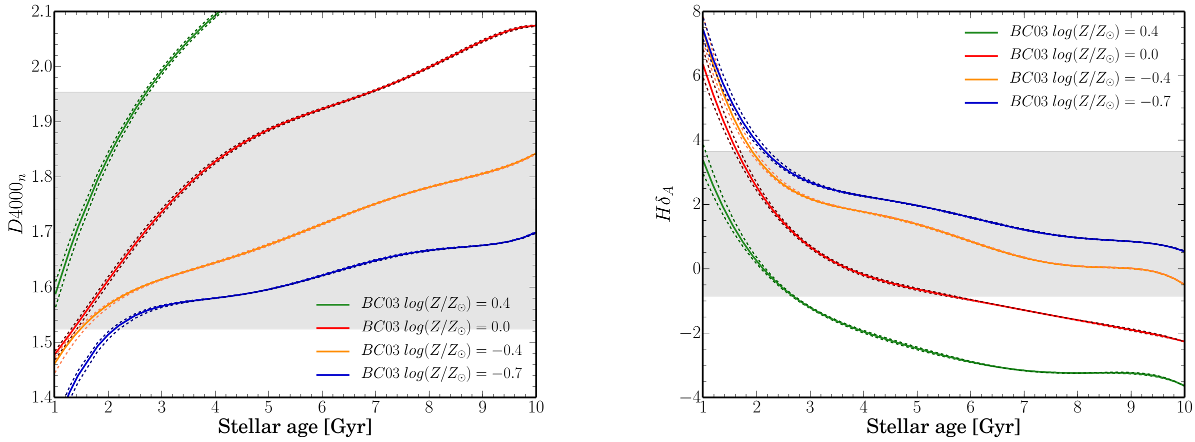

Fig. 1. $D4000_n$ ($H\delta_A$) – stellar age relation. Dashed lines correspond to $\tau = 0.1$, and 0.3 Gyrs, while the solid ones to $\tau = 0.2$ Gyr. Gray areas correspond to the ranges of $D4000_n$ and $H\delta_A$ measured on VIPERS stacked spectra of red passive galaxies. Reproduced from Siudek et al. (2017).

$\log(\mathrm{M_{star}/M_\odot})_{\mathrm{range}}$	$\log(\mathrm{M_{star}/M_\odot})_{\mathrm{med}}$	$log(Z/Z_\odot)_{med}$	$log(Z/Z_\odot)_{MAD}$
10.00-10.25	10.155	-0.039	0.003
10.25-10.50	10.405	-0.013	0.002
10.50-10.75	10.637	0.012	0.002
10.75-11.00	10.877	0.046	0.002
11.00-11.25	11.120	0.075	0.003
11.25-12.00	11.353	0.105	0.008

Table 1. The median stellar metallicities ($log(Z/Z_\odot)_{med}$) with uncertainties ($log(Z/Z_\odot)_{MAD}$) estimated for six $\mathrm{M_{star}}$ bins ($\log(\mathrm{M_{star}/M_\odot})_{\mathrm{range}}$) in the range of $10 < \log(\mathrm{M_{star}/M_\odot}) < 12$.

4 Results

4.1 The mass-metallicity relation for SDSS passive galaxies

In order to quantify the metallicity effect on measurements of spectral indices of red passive galaxy spectra, we first estimated the dependence of stellar metallicity on $\mathrm{M_{star}}$. To estimate the stellar metallicity range for VIPERS passive galaxies, we first checked the distribution of median metallicity as a function of $\mathrm{M_{star}}$ for 11,968 SDSS red passive galaxies (see left panel in Fig. 2). On average, we found somewhat super-solar metallicity for high-mass local passive galaxies. We expect that the median metallicity for the highest $\mathrm{M_{star}}$ bin ($\log(\mathrm{M_{star}}) \sim 11.3$ $\mathrm{M_\odot}$) would be not greater than $log(Z/Z_\odot) = 0.105 \pm 0.008$ (yellow star in left panel in Fig. 2 corresponds to the median values of stellar metallicities in different $\mathrm{M_{star}}$ bins). The median stellar metallicities for each of six analyzed $\mathrm{M_{star}}$ bins are listed in Tab. 1. The deviation from solar metallicity is expected to be relevant only at the high-mass end of VIPERS sample, which is populated by relatively older galaxies. For low-mass red passive galaxies with relatively low stellar ages ($\sim$ 2 Gyr) the effect of metallicity change ($log(Z/Z_\odot) = -0.039 \pm 0.003$ at $\log(\mathrm{M_{star}}) \sim 10.16$ $\mathrm{M_\odot}$) for both $H\delta_A$ and $D4000_n$ is minimal (see Fig. 1). Therefore, we ignored the metallicity effect for low-mass red passive galaxies in this work.

The estimation of the variations of stellar metallicity on $\mathrm{M_{star}}$ is in agreement with Gallazzi et al. (2014). Gallazzi et al. (2014) estimated the mean metallicity for passive high-mass (10^{11} $\mathrm{M_\odot}$) galaxies of $log(Z/Z_\odot) = 0.109 \pm 0.001$ and 0.07 ± 0.03 at the mean redshift $z = 0.1$ and $z = 0.7$, respectively, with a relatively flat slope.

Considering fixed metallicity at the level of solar metallicity, the observed change in $D4000_n$ between the high- and low-mass VIPERS red passive galaxies corresponds to the mean age difference of approximately 2 Gyr. On the other hand, the mean change of metallicity for the highest $\mathrm{M_{star}}$ bin at the level of 0.1 ($\log(\mathrm{Z/Z_\odot})$) results in the expected change of $D4000_n$ equal to ± 0.06 for galaxies with stellar age $\sim$ 4 Gyr. According to Gallazzi et al. (2014), the slope of the stellar metallicity-mass relation for passive galaxies equals to 0.15 ± 0.03 and

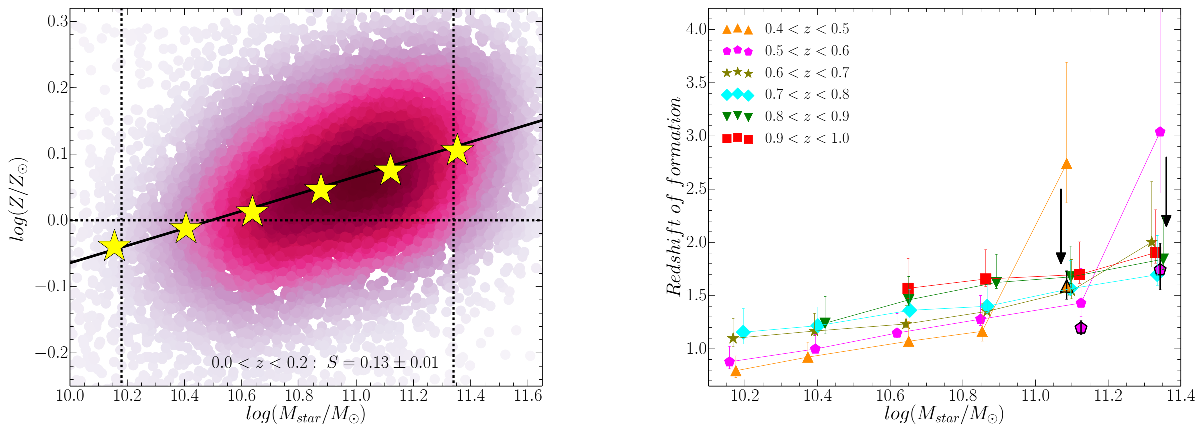

Fig. 2. Left: Stellar metallicity–mass relation for SDSS red passive galaxies. The linear fit is marked with a black, solid line. Yellow stars represent median values of stellar metallicity. The range of $M_{\rm star}$ analyzed in this paper is marked with black, dotted lines. The solar metallicity is marked with a horizontal, black, dotted line. **Right:** z_{form}–$M_{\rm star}$ relation for VIPERS red passive galaxies. Black arrows point the change in the value of z_{form} when solar and super-solar metallicity is considered for massive passive VIPERS galaxies.

0.11 ± 0.10 at z=0.1, and z=0.7, respectively. This is also confirmed by the relation found for the SDSS red passive galaxy sample, with a slope of 0.13 ± 0.01. Such a slope, and change in $D4000_n$, give a predicted slope of $D4000_n$-mass relation on the level of 0.07, and 0.10, again for z=0.1, and z=0.7, respectively. These values compose a significant fraction of the slope measured for the VIPERS sample ($S_D = 0.164 \pm 0.031$, Siudek et al. 2017). Thus, we can conclude that the $D4000_n$-mass relation changes because of the variation both in the age and metallicity of stellar populations in red passive galaxies, however, both effects cannot be clearly distinguished. The expected metallicity for VIPERS red passive galaxy sample is solar up to 10^{11} $M_{\odot}$ and then changes into the slightly super-solar metallicity of the order of 0.07 and 0.10 $\log(Z/Z_0)$ for the higher mass bins of $\sim 10^{11.1}$, $\sim 10^{11.4}$ $M_{\odot}$, respectively (see Tab. 1).

4.2 *The impact of metallicity on estimation of redshift of formation*

Neglecting small changes of galaxy metallicity with stellar mass may lead to a significant overestimation of redshift of formation for high-mass red passive galaxies. The slightly super-solar metallicities of 0.07 and 0.1 $log(Z/Z_{\odot})$ for $M_{\rm star}\sim 10^{11.1}$, and $\sim 10^{11.4}$ $M_{\odot}$, respectively, for passive galaxies should be considered.

The difference in redshift of formation for VIPERS red passive galaxies in the highest stellar mass bins derived from the analysis of $D4000_n$ and $H\delta_A$ with and without the metallicity effect are given in Tab. 2 and illustrated in the right panel in Fig. 2. This is especially important for two high-mass bins in the redshift range $0.4 < z < 0.6$, for which measured spectral indices are significantly stronger. In this case, the estimation of the epoch of the last starburst may be altered significantly, if the metallicity effect is neglected.

5 Conclusions

Redshift of formation strongly depends on the stellar metallicity variations with stellar mass. High-mass end ($> 10^{11}$ $M_{\odot}$) of red passive galaxies is characterized by slightly super-solar stellar metallicity ($log(Z/Z_{\odot}) \sim 0.1$). If solar metallicity is assumed, the z_{form} measurements are overestimated by 10-15%, but z_{form} might be even doubled for red passive galaxies observed within the redshift range of $0.4 < z < 0.6$. Therefore, it is essential to include metallicity effect when determining the epoch of the last starburst in high-mass ($> 10^{11}$ $M_{\odot}$) red passive galaxies.

We acknowledge the crucial contribution of the ESO staff for the management of service observations. In particular, we are deeply grateful to M. Hilker for his constant help and support of this program. KM, MS have been supported by the National Science Centre grants UMO-2013/09/D/ST9/04030 and UMO-2016/23/N/ST9/02963.

redshift	$\sim 10^{11.4}$ M$_\odot$ ($log(Z/Z_\odot = 0.1$)		$\sim 10^{11.4}$ M$_\odot$ ($log(Z/Z_\odot = 0.0$)	
	$D4000_n$	$H\delta_A$	$D4000_n$	$H\delta_A$
$0.4 < z < 0.5$	-	-	-	-
$0.5 < z < 0.6$	$1.74^{+0.25}_{-0.19}$	$2.19^{+0.58}_{-0.40}$	$3.04^{+1.72}_{-0.57}$	$4.09^{+8.73}_{-1.30}$
$0.6 < z < 0.7$	$1.54^{+0.10}_{-0.09}$	$1.78^{+0.34}_{-0.20}$	$2.00^{+0.57}_{-0.23}$	$2.43^{+1.55}_{-0.48}$
$0.7 < z < 0.8$	$1.49^{+0.08}_{-0.07}$	$1.66^{+0.14}_{-0.11}$	$1.70^{+0.37}_{-0.10}$	$1.86^{+0.43}_{-0.16}$
$0.8 < z < 0.9$	$1.63^{+0.09}_{-0.08}$	$1.81^{+0.20}_{-0.14}$	$1.84^{+0.39}_{-0.10}$	$2.01^{+0.62}_{-0.18}$
$0.9 < z < 1.0$	$1.68^{+0.09}_{-0.08}$	$1.81^{+0.20}_{-0.14}$	$1.90^{+0.40}_{-0.10}$	$2.00^{+0.68}_{-0.17}$
$0.4 < z < 1.0$	$1.62^{+0.12}_{-0.10}$	$1.85^{+0.29}_{-0.27}$	$2.10^{+0.69}_{-0.22}$	$2.48^{+2.40}_{-0.46}$

Table 2. Star formation epoch derived from the comparison of $D4000_n$ and $H\delta_A$ derived for the VIPERS high-mass passive galaxies with the corresponding values obtained from the BC03 model assuming solar metallicity (right panel) and SDSS-based super-solar metallicity ($log(Z/Z_\odot = 0.1$; left panel).

References

Balogh, M. L., Morris, S. L., Yee, H. K. C., Carlberg, R. G., & Ellingson, E. 1999, ApJ, 527, 54

Bruzual, G. & Charlot, S. 2003, MNRAS, 344, 1000

Carson, D. P. & Nichol, R. C. 2010, MNRAS, 408, 213

Fritz, A., Scodeggio, M., Ilbert, O., et al. 2014, A&A, 563, A92

Gallazzi, A., Bell, E. F., Zibetti, S., Brinchmann, J., & Kelson, D. D. 2014, ApJ, 788, 72

Gallazzi, A., Charlot, S., Brinchmann, J., White, S. D. M., & Tremonti, C. A. 2005, MNRAS, 362, 41

Gonzalez-Gonzalez, J. D. J. 1993, PhD thesis, University of California, Santa Cruz.

Guzzo, L., Scodeggio, M., Garilli, B., et al. 2014, A&A, 566, A108

Jones, L. A. & Worthey, G. 1995, ApJ, 446, L31

Kauffmann, G., Heckman, T. M., White, S. D. M., et al. 2003, MNRAS, 341, 33

Le Fèvre, O., Saisse, M., Mancini, D., et al. 2003, in Society of Photo-Optical Instrumentation Engineers (SPIE) Conference Series, Vol. 4841, Instrument Design and Performance for Optical/Infrared Ground-based Telescopes, ed. M. Iye & A. F. M. Moorwood, 1670–1681

Moresco, M., Pozzetti, L., Cimatti, A., et al. 2010, A&A, 524, A67

Osterbrock, D. E. 1989, Astrophysics of gaseous nebulae and active galactic nuclei

Scodeggio, M., Franzetti, P., Garilli, B., et al. 2005, PASP, 117, 1284

Scodeggio, M., Guzzo, L., Garilli, B., et al. 2018, A&A, 609, A84

Siudek, M., Małek, K., Scodeggio, M., et al. 2017, A&A, 597, A107

Thomas, D., Maraston, C., & Bender, R. 2003, MNRAS, 339, 897

Toft, S., Gallazzi, A., Zirm, A., et al. 2012, ApJ, 754, 3

Worthey, G. 1994, ApJS, 95, 107

Worthey, G. & Ottaviani, D. L. 1997, ApJS, 111, 377

The VIPERS Team coauthors: L. Guzzo[5,6], B. Garilli[7], M. Scodeggio[7], B. R. Granett[5,6], M. Bolzonella[8], S. de la Torre9, U. Abbas[10], C. Adami[9], D. Bottini[7], A. Cappi[8,11], O. Cucciati[12,8], I. Davidzon[9,8], P. Franzetti[7], A. Fritz[7], A. Iovino[6], J. Krywult[13], V. Le Brun[9], O. Le Fèvre[9], D. Maccagni[7], F. Marulli[12,14,8], M. Polletta[7,15,16], L.A.M. Tasca[9], R. Tojeiro[17], D. Vergani[18], A. Zanichelli[19], S. Arnouts[9,20], J. Bel[21], E. Branchini[22,23,24], J. Coupon[25], G. De Lucia[26], O. Ilbert[9], T. Moutard[27,9], M. Fumana[7], E. Jullo[9], A. Marchetti[7], C. Marinoni[21,28], H. J. McCracken[29], Y. Mellier[29], L. Moscardini[12,14,8], J. A. Peacock[30], W. J. Percival[31], G. Zamorani[8]; [5] Università degli Studi di Milano, via G. Celoria 16, 20133 Milano, Italy, [6] INAF - Osservatorio Astronomico di Brera, Via Brera 28, 20122 Milano – via E. Bianchi 46, 23807 Merate, Italy, [7] INAF - Istituto di Astrofisica Spaziale e Fisica Cosmica Milano, via Bassini 15, 20133 Milano, Italy, [8] INAF - Osservatorio Astronomico di Bologna, via Gobetti 93/3, I-40129, Bologna, Italy, [9] Aix Marseille Univ, CNRS, LAM, Laboratoire d'Astrophysique de Marseille, Marseille, France, [10] INAF - Osservatorio Astrofisico di Torino, 10025 Pino Torinese, Italy, [11] Laboratoire Lagrange, UMR7293, Université de Nice Sophia Antipolis, CNRS, Observatoire de la Côte dAzur, 06300 Nice, France, [12] Dipartimento di Fisica e Astronomia - Alma Mater Studiorum Università di Bologna, via Gobetti 93/2, I-40129, Bologna, Italy, [13] Institute of Physics, Jan Kochanowski University, ul. Swietokrzyska 15, 25-406 Kielce, Poland, [14] INFN, Sezione di Bologna, viale Berti Pichat 6/2, I-40127, Bologna, Italy, [15] Aix-Marseille Universit, Jardin du Pharo, 58 bd Charles Livon, F-13284 Marseille cedex 7, France, [16] IRAP, 9 av. du colonel Roche, BP 44346, F-31028 Toulouse cedex 4, France, [17] School of Physics and Astronomy, University of St Andrews, St Andrews KY16 9SS, UK, [18] INAF - Istituto di Astrofisica Spaziale e Fisica Cosmica Bologna, via Gobetti 101, I-40129 Bologna, Italy, [19] INAF - Istituto di Radioastronomia, via Gobetti 101, I-40129, Bologna, Italy, [20] Canada-France-Hawaii Telescope, 65–1238 Mamalahoa Highway, Kamuela, HI 96743, USA, [21] Aix Marseille Univ, Univ Toulon, CNRS, CPT, Marseille, France, [22] Dipartimento di Matematica e Fisica, Università degli Studi Roma Tre, via della Vasca Navale 84, 00146 Roma, Italy, [23] INFN, Sezione di Roma Tre, via della Vasca Navale 84, I-00146 Roma, Italy, [24] INAF - Osservatorio Astronomico di Roma, via Frascati 33, I-00040 Monte Porzio Catone (RM), Italy, [25] Department of Astronomy, University of Geneva, ch. dEcogia 16, 1290 Versoix, Switzerland, [26] INAF - Osservatorio Astronomico di Trieste, via G. B. Tiepolo 11, 34143 Trieste, Italy, [27] Department of Astronomy & Physics, Saint Mary's University, 923 Robie Street, Halifax, Nova Scotia, B3H 3C3, Canada, [28] Institut Universitaire de France, [29] Institute d'Astrophysique de Paris, UMR7095 CNRS, Université Pierre et Marie Curie, 98 bis Boulevard Arago, 75014 Paris, France, [30] Institute for Astronomy, University of Edinburgh, Royal Observatory, Blackford Hill, Edinburgh EH9 3HJ, UK, [31] Institute of Cosmology and Gravitation, Dennis Sciama Building, University of Portsmouth, Burnaby Road, Portsmouth, PO13FX.